Available online at www.sciencedirect.com
SCIENCE DIRECT®
International Journal of Pharmaceutics 298 (2005) 219–232
international journal of pharmaceutics
www.elsevier.com/locate/ijpharm

Pharmaceutical Nanotechnology

Micelle-like nanoparticles of PLA–PEG–PLA triblock copolymer as chemotherapeutic carrier

Subbu S. Venkatraman [a,*], Pan Jie [a], Feng Min [b], Boey Yin Chiang Freddy [a], Gan Leong-Huat [c]

[a] *School of Materials Science and Engineering, N4.1-1-30 Nanyang Avenue, Nanyang Technological University, Singapore 639798, Singapore*
[b] *Department of Applied Biology and Chemical Technology, Hong Kong Polytechnic University, Hung Hom, Kowloon, Hong Kong*
[c] *Natural Sciences and Science Education, National Institute of Education, Nanyang Technological University, Singapore 637616, Singapore*

Received 14 December 2004; received in revised form 8 March 2005; accepted 18 March 2005

Abstract

Triblock copolymer PLA–PEG–PLA were synthesized using ring opening polymerization with different LA/EG ratio. Micellar aggregates were prepared from these block copolymers and characterized. The degradation characteristics of selected copolymers were assessed in both micellar and film forms. Surface segregation of PEG was also quantified as a function of copolymer composition. Anti-cancer drugs 5-FU and paclitaxel were loaded into the micellar nanospheres with good efficiency. The drug release profile showed good control over the release of paclitaxel from these polymers.

Keywords: PLA; PEG; Drug carrier; 5-FU; Paclitaxel

1. Introduction

Micelle like nanoparticles are smaller than typical blood cells, such as erythrocytes or lymphocytes (ca. 7–10 μm), hence may be injected into the bloodstream. After intravenous injection, such particles may be able to achieve site- or tissue-specific delivery by exploiting physiological clearance mechanisms in the body. The drug incorporated in the particles is then released after the uptake of the nanoparticles inside the cells of the target tissue. Several advantages may be envisaged, such as dose reduction as a consequence of targeting, enhanced efficacy and reduced side effects. However, most particulate delivery systems are eliminated by the reticuloendothelial system (RES) within minutes, irrespective of their chemical composition, after intravenous injection. These particles accumulate in the liver and spleen following phagocytosis. For targeting

* Corresponding author. Tel.: +65 6790 4259; fax: +65 6790 9081.

0378-5173/$ – see front matter © 2005 Elsevier B.V. All rights reserved.
doi:10.1016/j.ijpharm.2005.03.023

to non-RES targets, such as tumor cells, avoidance of recognition by the RES is considered to be a major obstacle (Hagan et al., 1996; Gref et al., 1995).

To achieve long circulation time in blood and consequently localization in non-RES tissues, various attempts have been made, mainly by chemically attaching or adsorbing appropriate polymers or molecules on the particle surface, which would reduce or minimize the interaction with opsonins (Gref et al., 1994). Such particles constitute a so-called stealth therapeutic system. With stealth technologies, we can get the distribution of carrier systems to non-RES sites, and improve the immunospecific targeting strategies (Crommelin and Storm, 1998). Poly (ethylene glycol) PEG is widely used in this system (Storm et al., 1995; Okano et al., 1994).

A triblock copolymer of poly(lactic acid)-poly (ethylene glycol)-poly(lactic acid), PLA–PEG–PLA is a good candidate for achieving stealth characteristics, in addition to being biodegradable by hydrolysis. With the hydrophobic PLA (A) block and hydrophilic PEG (B) block, micelle-like nanoparticles can easily be obtained. The hydrophobic core can serve as reservoir for drugs and PEG shell play a dual role in stabilizing particles and dictating biodistribution of drugs.

Compared to poly(lactic-co-glycolic acid) (PLGA), microspheres prepared from these biodegradable block copolymers show striking differences in their release behavior for macromolecular model compounds, such as fluorescein isothiocyanate-linked Dextrans (FITC-dextrans) (M_w 400–500,000 g/mol). ABA polymers show a molecular mass dependent release, reminiscent of cross-linked hydrogels. Recently, paclitaxel was also encapsulated in PLA–PEG–PLA triblock copolymer (Ruan and Feng, 2003).

5-Fluorouracil (5-fluoro-2,4-pyrimidinedione) (5-FU) is a widely-used chemotherapeutic, but a problem with 5-FU therapy is its toxicity to the bone marrow and the gastrointestinal tract (Chabner, 1982). It has been recognized that, optimally, this drug should be dosed once or twice a week, preferably as a long-acting injectable and targeted to the desired site (Fu et al., 2002).

Paclitaxel, formulated in a 50:50 mixture of Cremophor® EL:absolute ethanol as Taxol™, is the world's most successful chemotherapeutic drug. However, Taxol™ also brings side effects such as dyspnea, flushing, rash and urticaria (Onetto et al., 1995). This hypersensitivity reaction is ascribed to the presence of the Cremophor® EL in the Taxol™. So it is necessary to find an alternative to the solubilizing agent. In this paper, a series of triblock copolymers with different molecular weight and LA/EG ratio have been synthesized and evaluated as drug delivery carriers for 5-FU and paclitaxel. The structure, thermal and degradation properties of the copolymers were characterized; micelle formation and surface compositions of the micelles were studied, and related to both degradation and drug release. We concentrate on the short-term degradation kinetics in this paper, as this is most relevant to the drug release profiles reported.

2. Materials and methods

2.1. Materials

L-Lactide, purchased from PURAC Far East Pte Ltd, was recrystallized three times from dry ethyl acetate and dried in vacuo at 40 °C for 12 h. Stannous octoate was purchased from Sigma and used without further purification. The poly (ethylene glycol) (Mn = 2000, 4000, 8000 Zur Synthese, Merck and Alderich), was dried at 120 °C for 6 h in vacuo, prior to use. Toluene was distilled over sodium and benzophenone was used as indicator for the dryness of the toluene. It was used until the color turned into purple. Ethyl acetate was distilled over P_4O_{10}. Other chemicals were used as received.

2.2. Experimental procedure

2.2.1. Synthesis of the copolymer

The L-lactide was first recrystallized from ethyl acetate, to remove the residual impurities in the monomer. The recrystallized lactide and dried PEG were transferred into a 250 ml pre-dried three-neck flask. Dry toluene was added into the three-neck flask followed by stannous octoate (0.05% (w/w), in toluene solution). The mixture was heated to 110 °C and allowed to reflux for 12 h. All syntheses were carried out under an oxygen- and moisture-free environment. The product was purified by repeated dissolution into dichloromethane and precipitation from cold ethyl

ether and ethanol. The isolated polymer was dried at 40 °C under vacuum.

2.2.2. Copolymer characterization

The copolymers were characterized by NMR. NMR studies were carried out on a Bruker 400 MHz instrument, operating at 400 MHz (^{1}H) and 100 MHz (^{13}C). $CDCl_3$ was used as solvent and TMS as internal reference.

Molecular weight (MW) and molecular weight distribution (MWD) of the polymers were determined using an Agilent series 1100 gel permeation chromatograph. A mixed bed column (PLGel Mixed Bed C, 5 μ, 300 × 7.5 mm, Polymer Laboratories), along with a guard column (50 × 7.5 mm, Polymer Laboratories), was employed. The mobile phase was a mixture of tetrahydrofuran (THF) and dichloromethane (DCM) in a volume ratio of 80:20. Molecular weights of samples were obtained relative to polystyrene standards. The flow rate was 1 ml/min and the temperature (both the column compartment and the flow cell of the refractive index detector) was 35 ± 0.1 °C.

The thermal properties of the polymer were studied using a modulated DSC (DSC 2920, TA Instuments, USA). The heating rate was 3 °C min^{-1}. The sample was then cooled at the rate of 10 °C per min to −60 °C and re-heated to 200 °C. Apparent melting temperatures were obtained from the endothermic peak and the enthalpy of fusion, from the area of the melting peak. The glass transition temperature (T_g) was determined from the second run.

2.2.3. Preparation of the micellar like nanoparticles with triblock copolymer

The copolymer was dissolved in 1 ml of organic solvent (acetone, THF, DMF (dimethyl formamide) or DMAC (dimethyl acetamide)) and then mixed with 20 ml of distilled water, under magnetic stirring. The solution was stirred overnight at 400 rpm/min to evaporate the organic solvent for acetone and THF, while for DMF and DMAC, the dialysis method was used to remove the organic solvent. In brief, as only those molecules smaller than the cut-off MW can diffuse through the dialysis membrane, the organic solvent was replaced by the dialysis medium (water) while the micelles remained inside the dialysis membrane. The micelle-like nanoparticles were obtained by freeze drying and kept in a desiccator.

2.2.4. Characterization of micellar particles

2.2.4.1. Examination of particle morphology. The surface morphology of the nanoparticles was observed using a JEOL JSM-6340F field emission scanning electron microscope (FESEM) at 5.0 kV. The samples were mounted on a metal holder using double-sided copper tape, and then coated with gold using a pulse plasma system before observation.

2.2.4.2. Determination of particle size. The measurement of the particle size distribution was carried out by BI-MAS (multi angle sizing option on the Zetaplus, Brookhaven Instruments Corporation). All measurements were performed at 25 °C at a measurement angle of 90 °C, in triplicate. The measurement yields a hydrodynamic diameter for the particles.

2.2.4.3. Critical micelle concentration (CMC) and stability of the micelle to added electrolyte. The critical micelle concentration (CMC) of the copolymers was determined by fluorescence spectroscopy using pyrene as fluorescence probe. Upon formation of micelles, pyrene would move into the inside of the micelles from the aqueous phase which results in an alteration in the intensity ratio (I_1/I_3) of pyrene fluorescence bands I (371 nm) an III (383 nm).

The effect of the added electrolyte to the aggregation behavior was studied using the method reported by Riley et al. (1999), by adding 0.5 ml of each colloidal dispersion to 2.5 ml of Na_2SO_4 solutions of varying concentration (0–0.8 M), and measuring the turbidity at a wavelength of 500 nm after 15 min (Shimadzu UV-2501 PC, UV–vis Recording Spectrophotometer). The critical flocculation point (CFPT) was taken as the electrolyte concentration at which a dramatic increase in the turbidity was first detected. The reversibility of this process was assessed by diluting the flocculated dispersion with water and assessing if the flocs could be redispersed with agitation.

2.2.5. Determination of surface composition

XPS measurements were carried out on a VG Scientific ESCA LAB Mk II spectrometer equipped with an Mg Kα X-ray source (1235.6 eV photons) and a hemispherical energy analyzer. The copolymer samples were analyzed in film and particle form. For films, solutions were spin-coated on pre-cleaned glass slides.

After removing the solvent in vacuum, they are tested by XPS. For particles, the freeze-dried nanoparticles (ALPHA 1–4 LSC, Christ GmbH) were mounted on the glass slide with the help of double-side adhesive tape. The tape was fully covered by the freeze dried nanoparticles.

A series of survey spectra were recorded over a binding energy range of 0–1000 eV using passive energy 20 eV. In all cases the survey spectra recorded the presence of only oxygen (O1s 533 eV) and carbon (C 1s 285 eV) at the surface. Detailed analysis of C 1s regions of each sample was recorded over a binding energy range of 280–300 eV. Charge referencing was performed using the C–H peak (285.0 eV) for PLA–PEG–PLA samples. The curve fitting was performed by the computer program Kratos provided by the equipment manufacturer. A Gaussian–Lorentzian function was applied to all data. No asymmetry component was introduced.

2.2.6. In vitro degradation of polymer films

Polymer films cast from 5% (w/v) DCM solutions on Teflon® plates with the help of automatic film applicator (Gardner, AG-2150), were allowed to dry for 72 h. Residual solvents were then removed in vacuum at room temperature for 2 days. Films were cut into 2 cm × 2 cm slabs with a thickness of around 50 μm. The samples were totally immersed in 30 ml of isotonic phosphate buffered saline solution (PBS, pH 7.4, Sigma) in sealed bottle and equilibrated in a water bath in 37 °C. At certain time intervals, samples were withdrawn and dried in vacuum until constant weight was reached. Changes of the molecular weights (GPC), film morphology (FESEM), thermal properties (MDSC) and chemical structure (NMR) were investigated. For selected copolymers, micelle-like nanoparticles were also degraded for comparison to films.

2.2.7. In vitro drug release from micelle like nanoparticles

2.2.7.1. 5-FU. Copolymer and drug at a certain ratio were both dissolved in 3 ml DMF. This solution was added dropwise into 15 ml of deionized water under medium magnetic stirring. After dialysis to remove DMF (Medicell International Ltd. MWCO 12,000–14,000 Da), the suspension was centrifuged to remove the water. The liquid removed from the dialysis and centrifuge, was carefully collected and the free drug amount was obtained from the concentration of the drug in the liquid. 1 ml PBS was added into the remaining residue and the colloidal solution was placed into dialysis membrane again. The membrane was placed in bottles with 10 ml PBS (pH 7.4) in an incubator at 37 °C. At a fixed time interval, the release medium was replaced by 10 ml fresh PBS. The concentration of released drug was determined by its absorbance at 266 nm (Shimadzu UV-2501PC). The cumulative released amount of 5-FU was calculated by the concentration and volume of the solution medium.

2.2.7.2. Paclitaxel. The copolymer and paclitaxel with certain ratio were both dissolved in DMF. The clear solution was dropwise added into the 10 ml deionized water with mild magnetic stirring. The colloidal solution was centrifuged at 50,000 × *g* for 2 h (4 °C, Jounan® KR25i) to remove the supernatant containing free drug and organic solvent. The residue was redispersed into 3 ml deionized water and divided into three equal portions. 1 ml solution was added into 3 separate centrifuge tubes containing 9 ml PBS and put into 37 °C water bath. The release medium was replaced at certain time interval and HPLC was used to quantify the paclitaxel.

Reverse-phase HPLC was used to quantify the amount of paclitaxel released from the copolymer micelles. The chromatographic analysis is performed on an Agilent 1100 Series instrument equipped with a VW detector and a ZORBAX 300SB-C18 column. The operating conditions were as follows: sample volume, 20 μl; mobile phase flow-rate, 1.0 ml/min; λ = 227 nm. An amount of 50/50 (v/v) acetonitrile/water is used as mobile phase. Calibration curve was run with paclitaxel/acetonitrile solution with different paclitaxel concentrations:

$$\text{theoretical drug content (\%)} = \frac{\text{mass of drug used in formulation}}{\text{mass of copolymer and drug in formulation}} \times 100,$$

$$\text{drug entrapment (\%)} = \frac{\text{mass of drug in particles}}{\text{mass of drug used in formulation}} \times 100,$$

Table 1
$PLA_x/PEG_y/PLA_x$ triblock copolymers obtained from polymerization of L-lactide

Copolymer	^{1}H-NMR				GPC	
	LA/EG in feed	LA/EG in product[a]	DP_{PLA}	M_n ($PLA_x/PEG_y/PLA_x$)	M_n[b] ($PLA_x/PEG_y/PLA_x$)	M_w/M_n[c]
PLA_{17}–PEG_{91}–PLA_{17}	0.50	0.37	17	6480	7940	1.07
PLA_{61}–PEG_{91}–PLA_{61}	1.52	1.34	61	12710	13280	1.10
PLA_{68}–PEG_{91}–PLA_{68}	2.09	1.47	68	13710	14680	1.11
PLA_{90}–PEG_{91}–PLA_{90}	2.49	1.98	90	17940	17310	1.12
PLA_{41}–PEG_{45}–PLA_{41}	2.05	1.82	41	7950	10520	1.11
PLA_{97}–PEG_{45}–PLA_{97}	4.52	4.26	97	15940	22800	1.19
PLA_{62}–PEG_{182}–PLA_{62}	0.95	0.68	62	16900	15690	1.22

[a] LA/EG in product and DP_{PLA} are determined from the integration ratio of resonance due to PEG blocks at 3.64 ppm (–O–CH_2–CH_2–) and to the PLA blocks at 5.17 ppm (Me–CH^*<) in the ^{1}H-NMR. $DP_{PEG} = 4000/44 = 91$, $DP_{PLA} = DP_{PEG}{}^*$(LA/EG)/2.
[b] Based on polystyrene standards.
[c] Polydispersities of copolymer are determined from GPC, it is the ratio of weight average molecular weight (M_w) and number average molecular weight (M_n).

$$\text{drug content (\%)} = \frac{\text{mass of drug in nanoparticles}}{\text{mass of nanoparticles recovered}} \times 100,$$

$$\text{nanoparticle recovery (\%)} = \frac{\text{mass of nanoparticles recovered}}{\text{mass of polymer, drug and any excipient used in formulation}} \times 100.$$

3. Results and discussion

3.1. Synthesis and purification of the copolymer

A series of PLA–PEG–PLA block copolymer have been synthesized. From Table 1, it could be found that with the increase of the LA/EG in feed ratio, the molecular weight of the copolymer increased as expected. The number average molecular weights of the ABA

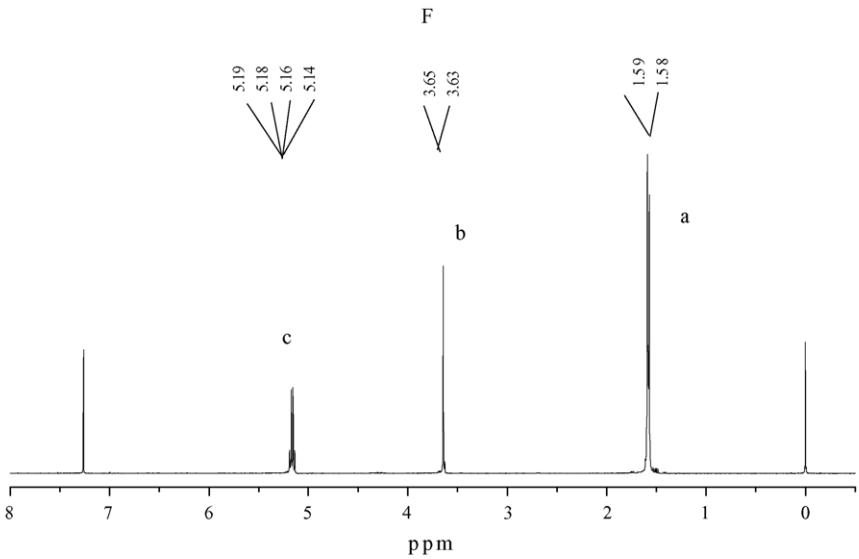

Fig. 1. ^{1}H-NMR spectrum ($CDCl_3$) of the copolymer.

block copolymers ranged from 6400 to 18000 and the molecular weight distribution are narrow, as seen in Table 1.

3.2. Structure characterization

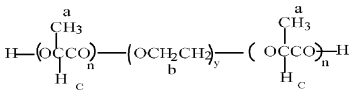

In Fig. 1, a typical ^{1}H-NMR spectrum is shown. The presence of methine (CH) and methyl (CH_3) protons in PLA was observed at around 5.17 ppm (c) and 1.60 ppm (a) respectively. Tetralet and doublet split peaks were observed. The methene protons in CH_2 group of PEG were around 3.64 ppm.

The ^{13}C-NMR spectra (not shown) of the synthesized copolymer is used to confirm the PLA blocks, by noting the presence of the C=O, CH and CH_3 groups in the PLA block at 170.0, 69.4 and 17.0 ppm, respectively. The CH_2 group in PEG block could be found at 71.0 (b) ppm.

3.3. Thermal analysis

The homopolymers PLLA (I.V. = 1.04) and PEG 2 k, 4 k, 8 k were studied for comparison to the triblock copolymers. Thermal data are summarized in Table 2. The copolymers show two distinct melting peaks for the PLA and PEG, indicating good microphase separation. The presence of the PLA sequences attached to PEG blocks decreased the melting temperature of both the PEG block and PLA block. It can be found that in the presence of relatively long PLA chain, short PEG segments (PLA_{41}–PEG_{45}–PLA_{41}, PLA_{91}–PEG_{45}–PLA_{91}) do not crystallize, which agrees with the results of S.M Li et al. (1996) (Rashkov et al., 1996). Similarly, for copolymers with longer PEG segments (PLA_x–PEG_{91}–PLA_x), crystallinity is found for PEG only when the LA segment is short (PLA_{17} and PLA_{61} only). As for the PLA blocks, for a given PEG segment length, both the T_m and the DC increase with increasing PLA length. It should be noted that PLA also has a T_g just at about 50 °C, which is close to the T_m of PEG.

3.4. Hydrolytic degradation of triblock copolymer

For the application of those biodegradable polymers as drug delivery carriers, it is very important to know the degradation profiles. The long-term (up to 90 weeks) degradation characteristics have been studied (Hu and Liu, 1994; Li et al., 1998), but not the details of the shorter-term profile (1–3 weeks), which is more important for drug release prediction of common chemotherapeutics. In this paper, four different triblock copolymers were chosen to study the degradation properties within the first 3 weeks, in relation to the drug release profile. For one copolymer (PLA_{90}–PEG_{91}–PLA_{90}), the degradation was studied for both film and particle forms.

The MW data for the four polymers in film forms are compared in Fig. 2, while Fig. 2 shows how the MWD changes with degradation of two representative polymers.

Table 2
Thermal properties of triblock copolymers

Sample	LA/EG ratio	T_m (PEG) (°C)	T_m (PLA) (°C)	ΔH_m (J/g)	T_c(PLA) (°C)	ΔH_c (J/g)	DC (%)	T_g (°C)
PLLA	–		177.5					54
PLA_{17}–PEG_{91}–PLA_{17}	0.4	37.3	–	–	–	–	–	–
PLA_{61}–PEG_{91}–PLA_{61}	1.3	42.5	141.4	34.9	–	–	37.3	−2.7
PLA_{67}–PEG_{91}–PLA_{67}	1.5	–	148.7	45.7	95.7	11.1	37.0	−1.4
PLA_{90}–PEG_{91}–PLA_{90}	2.0	–	153.8	47.9	102.2	8.3	42.3	−0.7
PLA_{41}–PEG_{45}–PLA_{41}	1.8	–	146.5	43.4	93.6	1.7	46.3	−0.1
PLA_{97}–PEG_{45}–PLA_{97}	4.3	–	162.3	61.1	108.3	11.5	53.4	−3.1
PLA_{62}–PEG_{182}–PLA_{62}	0.7	48.5	150.3	23.6	88.6	5.8	19	−1.2
PEG (2000)		50.4						–
PEG (4000)		59.6						−0.8
PEG (8000)		59.8						3.5

DC = degree of crystallinity of PLA block, rating it to the reference 100% crystalline L–PLA (93.6 J/g) (Leenslag et al., 1984).

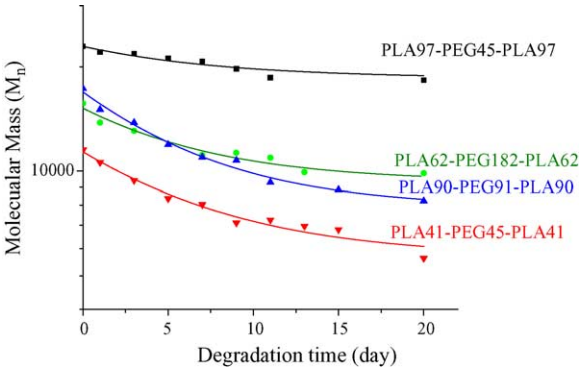

Fig. 2. Molecular weight changes as a function of time.

We find two distinct patterns of degradation, as seen from the MWD. From Fig. 3, it can be seen that both copolymers initially exhibited a monomodal molar mass distribution. However, two of the copolymers PLA_{62}–PEG_{182}–PLA_{62} (not shown) and PLA_{90}–PEG_{91}–PLA_{90} (Fig. 3(a)) showed bimodal profiles while copolymers with shorter PEG blocks (PLA_{97}–PEG_{45}–PLA_{97}, Fig. 3(b) and PLA_{41}–PEG_{45}–PLA_{41}, not shown) showed no obvious bimodal profile after 20 days of degradation. It was found the ratio of the new peak increased with the time of degradation. Li et al. (1998) reported bimodality in all the triblocks studied, which varied in LA to EG ratio from about 1–5. However, in their work, the second peak appeared only after about 11 weeks in 3 of the polymers, and after 25 weeks for the polymer with a LA/EG ratio of 5. Moreover, the PEG block length was kept constant at 41 in their studies.

In our work, we observe bimodality within 20 days, for all triblocks with PEG lengths above 90 DP. The mechanism proposed by Li et al. is that the bimodality is a consequence of the different rates of hydrolysis in the crystalline (or crystallisable) phase of PLA blocks. In this study, we have used four polymers, all with initial crystallinity, and two of comparable initial crystallinity; yet we find that bimodality sets in early only for those copolymers with long PEG blocks. This might

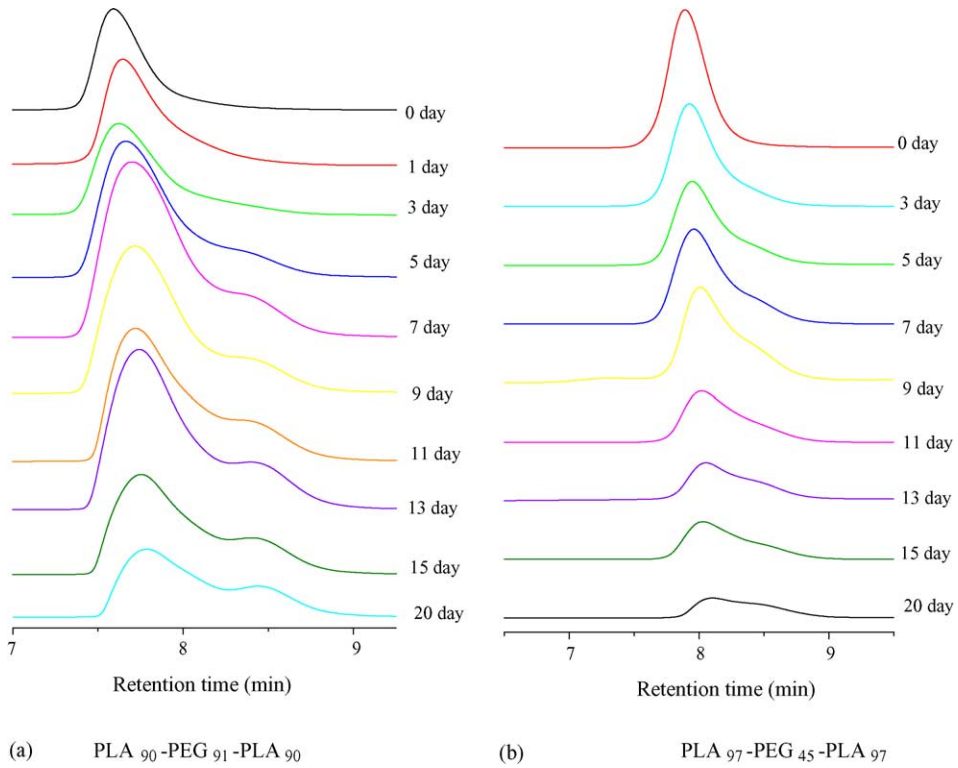

Fig. 3. GPC chromatograms of series of PLA–PEG–PLA triblock copolymers with degradation.

Table 3
LA/EG ratios of the copolymers at different degradation time

Degradation time (day)	0 day	20 day
PLA_{41}–PEG_{45}–PLA_{41}	1.8	1.8
PLA_{97}–PEG_{45}–PLA_{97}	4.3	4.1
PLA_{90}–PEG_{91}–PLA_{90}	1.8	1.7
PLA_{62}–PEG_{182}–PLA_{62}	0.7	0.6

be due to faster water ingress for those copolymers with longer PEG chains.

NMR provides a means to examine, at least qualitatively, the composition changes of the degrading copolymer. It was found from the ^{1}H-NMR spectra that all the copolymers showed a very slight decrease in LA/EG ratio after 20 days. This certainly indicates very little loss of either EG- or LA-containing groups up to 20 days (Table 3), further substantiating our earlier explanation for bimodality.

Thermal property changes were also investigated by MDSC. For all the copolymers, the melting peak of PLA block decreased with the degradation time. It can be found in Fig. 4 that, for triblock copolymers with a relatively long PLA chain, T_m decreased slowly in the first 20 days, whereas for the copolymer with relatively short PLA chain, T_m decreased faster initially. The decrease in T_m attests to attack on the crystalline regions.

Finally, we compare the degradation profiles of the same polymer in particle and film forms, using PLA_{90}–PEG_{91}–PLA_{90} and PLA_{97}–PEG_{45}–PLA_{97} as an example (Fig. 5A and B). For PLA_{90}–PEG_{91}–PLA_{90}, this polymer exhibits bimodality when degrading in film form after about 7 days, but the bimodality is much less pronounced in nanoparticle form, although MW reduction rates are comparable. This can only be attributed to the fact that thickness plays a role in enhancing the heterogeneity of MW reduction. In other words, in the thicker film, the degradation in the interior of the film is substantial, and the low-MW species are retained in the interior, whereas at the surface, the low-MW 'tail', when generated, leaches out. Moreover, when the film form does not exhibit any bimodality, neither does the nanoparticle form, as seen with PLA_{97}–PEG_{45}–PLA_{97}. The divergence between PLA_{90}–PEG_{91}–PLA_{90} and PLA_{97}–PEG_{45}–PLA_{97} in the trend of molecular weight loss in nanoparticle form might be the combined result caused by the EG chain length, the water uptake and particle size.

We have also shown, by XPS (see below), that there is no surface segregation of PEG segments for particles or for films of PLA_{90}–PEG_{91}–PLA_{90}, thus reinforcing the more heterogeneous nature of the degradation for films is purely a consequence of the thickness of the film.

3.5. Preparation and morphology of nanoparticles

Micelle-like nanoparticles prepared from PLA–PEG–PLA triblock have already been studied by many research groups (Nakada et al., 1998; Matsumoto

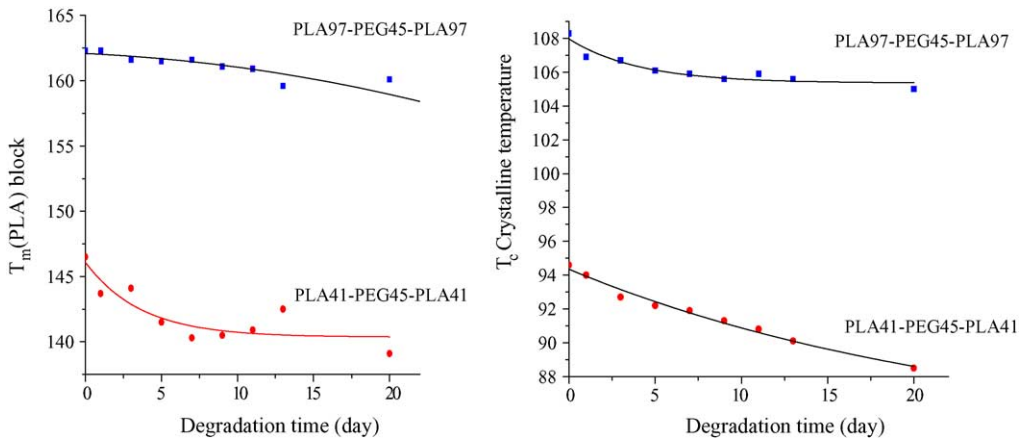

Fig. 4. Melting and crystalline temperature change with the degradation time.

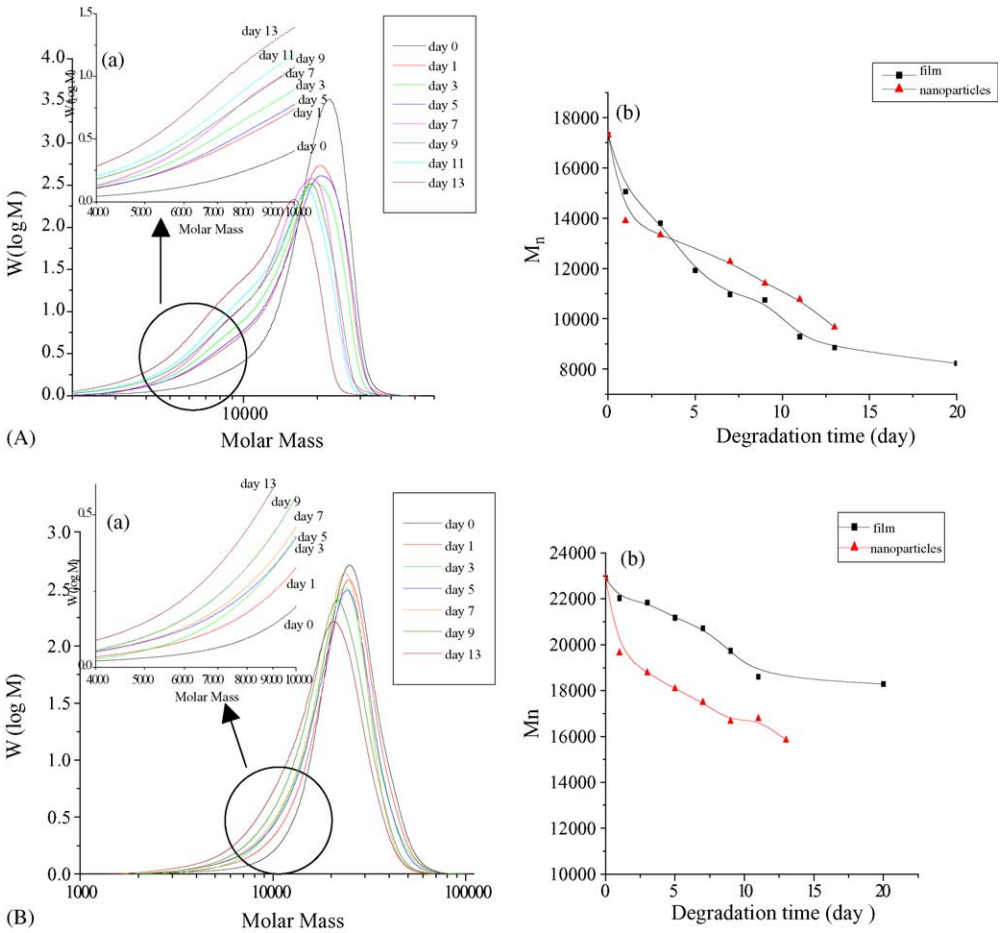

Fig. 5. (A) Comparison of degradation data for nanoparticles and film of PLA_{90}–PEG_{91}–PLA_{90} (a) GPC chromatograms of nanoparticles and (b) molecular weight loss. (B) Comparison of degradation data for nanoparticle and film of PLA_{97}–PEG_{45}–PLA_{97} (a) GPC chromatograms of nanoparticles and (b) molecular weight loss.

et al., 1999; Jaeghere et al., 2000). The solvent evaporation method is most widely used and acetone is the most common solvent used to prepare nanoparticles, as it is miscible with water and can be easily evaporated. However, we have found that DMF is a better choice than THF and acetone in terms of gettting particles in the nanometer range, and have used the dialysis method to exchange it for water.

The freeze dried nanoparticles were observed with FESEM (Fig. 6). This image was typical of those obtained for all the samples, confirming that the PLA–PEG–PLA copolymers form spherical, discrete particles in aqueous media.

3.5.1. *Particle size and stability study*

The hydrodynamic diameter of particles is determined by DLS (dynamic light scattering). The effective diameter and polydispersity of particulate dispersions are presented in Table 4.

The effect of the different PLA and PEG segments length on the particle sizes is also seen in Table 4. It can be found that for the series of PLA_x–PEG_{91}–PLA_x, with the increase of the PLA segments length, the particle sizes also increased. The longer the PLA segments are, the larger the hydrophobic cores formed. However for PLA_x–PEG_{45}–PLA_x series, the chain length of PLA block has little effect on the particles size.

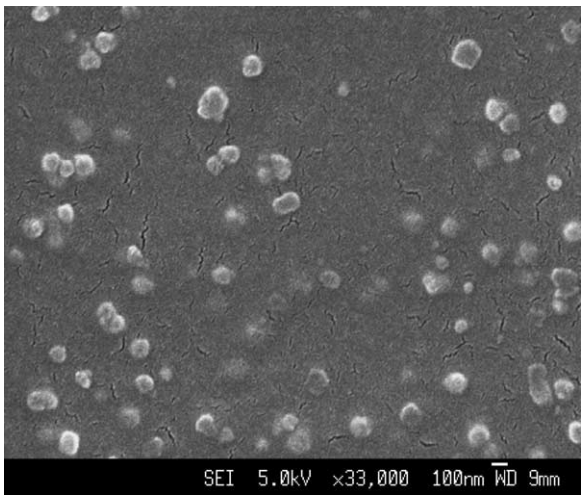

Fig. 6. FESEM micrographs of PLA_{61}–PEG_{91}–PLA_{61} micelle like nanoparticles.

Critical micelle concentration (CMC) and the critical flocculation point (CFPT) are two important stability indicators for micelles. With the increase of concentration of the copolymer, the block copolymer forms multi-molecular micelles and micelle aggregates.

Plots of I_1/I_3 band intensity ratio of pyrene monomer as a function of PLA–PEG–PLA copolymer concentration can be used to determine the CMC. Below the CMC, the I_1/I_3 value is nearly constant. Above this concentration, this value decreases with increasing concentration, which indicated partitioning of this hydrophobic probe between the hydrophobic core of micelle and aqueous phase. From the results, it could be found that with the increase of the PLA chain length, the CMC also increased. This implies that the shorter the hydrophobic block, the easier it is for the micelle to form.

When the ionic strength of the medium is increased, aqueous dispersions flocculate because of the net breakdown of the hydrogen bonding between the polymeric ether oxygen or OH groups and the surrounding water molecules (Tadros and Vincent, 1980). This behavior is of significance for intravenous injection. Riley et al. (1999) also studied the stability of micelle-like PLA–PEG nanoparticles with different PLA chain lengths. We find, as Riley et al. did, that the CFPT decreased greatly as the chain length of the PLA block was increased. The main reason for this instability could be the larger-sized particles obtained with longer PLA segments, with the consequent lower PEG surface coverage.

3.5.2. Surface chemistry

XPS analysis can provide quantifiable data on biomaterial surface chemistry. Gref et al. (1994) used XPS to study the surface composition of the nanopspheres of PLGA-mPEG diblock copolymer. They found most of the PEG is concentrated within 5 nm of the outer layer of the nanospheres. However, Ruan and Feng (2003), found that the distribution of PEG segments was homogenous in the PLA–PEG–PLA microspheres, which was different from the diblock copolymer PLA-mPEG nanoparticles (Kim et al., 2001a,b), in which the hydrophilic PEG migrated to the surface. We found that surface composition of the triblocks were dependent on the overall composition (Tables 5A and 5B). Copolymers with longer PLA chain lengths, such as PLA_{90}–PEG_{91}–PLA_{90} have homogenous PEG distribution, whereas for copolymers with shorter PLA chains, such as PLA_{61}–PEG_{91}–PLA_{61}, the nanoparticles have the higher PEG surface concentration than bulk copolymer. This implies surface segregation of PEG blocks, i.e. PEG attached to shorter PLA segments simply find it easier to migrate to the surface.

Table 4
Hydrodynamic diameter, polydispersity and stability of PLA–PEG–PLA micelles

	Particle size mean ± S.D. (nm)	Polydispersity (mean ± S.D.)	CMC (mg/ml)	CFPT (mol/L)
PLA_{61}–PEG_{91}–PLA_{61} (20 mg/ml, in DMF)	63.8 ± 3.0	0.31 ± 0.03	0.0024	0.55
PLA_{68}–PEG_{91}–PLA_{68} (20 mg/ml, in DMF)	138.0 ± 0.5	0.21 ± 0.01	0.0042	0.55
PLA_{90}–PEG_{91}–PLA_{90} (20 mg/ml, in DMF)	210.7 ± 0.5	0.25 ± 0.01	0.0046	0.50
PLA_{62}–PEG_{182}–PLA_{62} (20 mg/ml, in DMF)	168.8 ± 1.3	0.26 ± 0.01	0.0070	0.55
PLA_{41}–PEG_{45}–PLA_{41} (20 mg/ml, in DMF)	93.3 ± 1.3	0.19 ± 0.08	n.d.	0.50
PLA_{97}–PEG_{45}–PLA_{97} (20 mg/ml, in DMF)	93.8 ± 0.3	0.20 ± 0.01	n.d.	0.20

Table 5A
XPS data for particle and film of PLA_{90}–PEG_{91}–PLA_{90}

Peak	Pure copolymer			Nanoparticles	
	Binding energy (eV)	Theoretical (%)	Experimental (%)	Binding energy (eV)	Experimental (%)
a	284.995	22.68	22.22	285.009	21.16
c	287.327	22.68	22.22	287.119	23.01
d	289.241	22.69	22.98	289.258	23.44
b	286.150	31.95	32.57	286.050	32.39

Table 5B
XPS data (1s regions) for particle and film of PLA_{61}–PEG_{91}–PLA_{61}

Peak	Pure copolymer			Nanoparticles	
	Binding energy (eV)	Theoretical (%)	Experimental (%)	Binding energy (eV)	Experimental (%)
a	285.000	19.09	19.11	285.000	17.88
c	287.370	19.09	19.11	287.470	17.72
d	289.243	19.08	19.12	289.656	16.08
b	286.254	42.74	42.66	286.344	48.32

Table 6
Hydrodynamic diameter, polydispersity of PLA–PEG–PLA nanoparticles w/o drug

	Particle size (nm) mean ± S.D. (without drug)	Particle size (nm) mean ± S.D. (with drug)	Polydispersity mean ± S.D. (without drug)	Polydispersity mean ± S.D. (with drug)
PLA_{61}–PEG_{91}–PLA_{61}	63.8 ± 3.0	75.0 ± 6.1	0.31 ± 0.03	0.17 ± 0.04
PLA_{68}–PEG_{91}–PLA_{68}	138.0 ± 0.5	179.1 ± 20.0	0.22 ± 0.01	0.22 ± 0.01
PLA_{90}–PEG_{91}–PLA_{90}	210.7 ± 0.5	219.4 ± 1.7	0.25 ± 0.01	0.24 ± 0.01

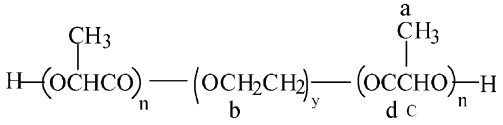

These data clearly show that in order to generate stable particles with potential ‘stealth’ capability, we need to use particles made from long PEG and short PLA segments, such as PLA_{61}–PEG_{91}–PLA_{61}. We are currently evaluating the interactions of these particles with macrophages in vitro.

3.6. In vitro drug release

After drug incorporation, particle sizes change somewhat, as shown in Tables 6 and 8A. The size distribution is narrow. It could also be seen from Table 7, that the efficiency of drug entrapment was greatly affected

Table 7
Effect of different PLA block chain length on 5-FU drug entrapment

	Different copolymer[a]			Different polymer/drug ratio[b]		
	PLA_{61}–PEG_{91}–PLA_{61}	PLA_{68}–PEG_{91}–PLA_{68}	PLA_{90}–PEG_{91}–PLA_{90}	Polymer/drug = 10:1	Polymer/drug = 10:2	Polymer/drug = 10:5
Theoretical drug loading (%)	9.1	9.1	9.1	9.1	16.7	33.4
Drug entrapment (%)	14.2	15.5	12.6	13.1	19.7	38.8

[a] The polymer/drug ratio maintained at 10:1.
[b] PLA_{68}–PEG_{91}–PLA_{68} was used in this research.

Table 8A
Particle size of drug loaded and blank micelle-like nanoparticle

Copolymer	Blank (nm) particle size ± S.D.	100 μg (nm) particle size ± S.D.	300 μg (nm) particle size ± S.D.	500 μg (nm) particle size ± S.D.
PLA_{90}–PEG_{91}–PLA_{90}	133 ± 1.0[a]	145 ± 0.8	145 ± 0.9	147 ± 0.7

[a] The polymer concentration in DMF is 10 mg/ml.

Table 8B
Drug entrapment efficiency of nanoparticles prepared with triblock copolymer with different polymer drug feed ratio

	Taxol in feed (μg)	Nanoparticle recovery (%)	Theoretical drug loading (%)	Drug content (%)	Entrapment Efficiency (%)
PLA_{90}–PEG_{91}–PLA_{90}	100.00	41.82	1.00	0.13	13.55
	300.00	69.71	3.00	0.76	25.87
	500.00	72.79	5.00	1.54	31.41

by the initial polymer/drug concentration ratio while the chain length of PLA block had little effect.

3.6.1. Drug release data

3.6.1.1. 5-FU. The solubility of 5-FU in water is about 12.5 mg/ml, so it is not a hydrophobic drug. 5-FU was continuously released *in vitro* over 300 h. The rate of release was high, in accordance with other work (Avgoustakis et al., 2002; Kim et al., 2001a,b). From Fig. 7, it is clear that the release profiles for nanoparticles made from different block copolymer were nearly the same. Basically, there is not much control over the release rate for this drug.

Most of the drug is released within 2 to 3 days, by diffusion and burst; there is perhaps a later degradation-controlled release for a small fraction of the drug. We believe that this profile is due to the hydrophilic nature of the drug which does not permit encapsulation in the micelle core.

3.6.1.2. Paclitaxel. When a very hydrophobic drug, such as paclitaxel, is incorporated into these micelle-like particles with a hydrophobic core, much better control is obtained over the release. First, at lower theoretical drug loading (1–5%), the drug entrapment efficiency remains comparable to 5-FU with high theoretical drug loading (9–33%), as seen in Table 8B. Second, the drug release rate is much lower, and complete release of drug is accomplished only after 12 days (Fig. 8). Interestingly, the release profile is indicative of diffusion-controlled release only over this time period.

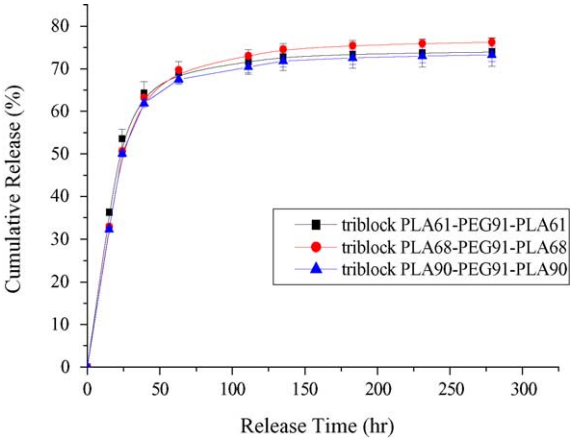

Fig. 7. Release profile of 5-FU from nanoparticles of triblock copolymer PLA–PEG–PLA with different PLA blocks.

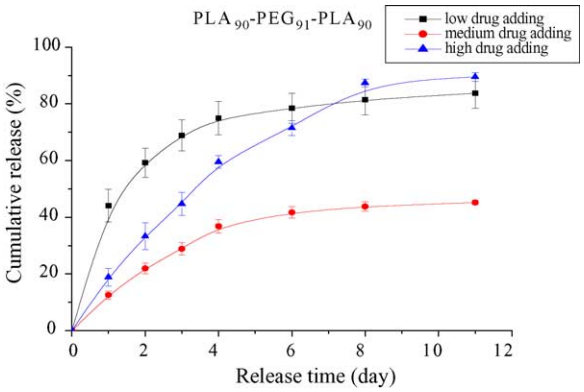

Fig. 8. Release of paclitaxel from PLA_{90}–PEG_{91}–PLA_{90} nanoparticles.

In comparison to reported data on similar systems (Ruan and Feng, 2003; Liggins and Burt, 2002; Burt et al., 1999), we find that the release rate from our triblock copolymer is faster compared to the nanoparticle release reported by Ruan. Reasons for the discrepancy may be the lower particle size in our work (210 nm) compared to Ruan's (20 microns); the size difference may also explain the relatively higher encapsulation efficiency reported in Ruan's work. Somewhat in agreement with Ruan, we find an inverse dependence of release rate on drug loading, i.e., lower loadings appear to have faster rate of release.

4. Conclusions

PLA–PEG–PLA triblock copolymers were synthesized by a ring-opening reaction of L-lactide with PEG using stannous octoate as catalyst. Thermal properties of these polymers indicate that the PLA and PEG phase separate into separate crystalline domains; however, when compared to pure PLA polymer, these copolymers all degrade faster, presumably due to higher hydrophobicity.

The details of the MWD during degradation reveal some interesting trends. The copolymers PLA_{62}–PEG_{182}–PLA_{62} and PLA_{90}–PEG_{91}–PLA_{90} show bimodal profiles within 20 days of degradation, while the other copolymers do not. We believe that the bimodality is due to heterogeneous degradation occurring within 20 days for these copolymers, due to a faster rate of water ingress.

Micelle-like nanoparticles were prepared with the ABA triblock copolymers using solvent-evaporation and solvent-dialysis method. It was found that DMAC and DMF were better solvents in terms of obtaining the nanoparticles than acetone and THF. For the PLA_x–PEG_{91}–PLA_x series, particle sizes increased with increasing PLA segment length. With the increase of the PLA chain length, the CMC also increased, indicating greater difficulty of micelle formation. Moreover, such micelles are also less stable to flocculation, which we attribute to overall less PEG surface coverage. XPS measurements show that surface segregation of PEG is found only when PLA segment length is relatively small (DP of PLA $\sim$ 60 or less), clearly indicating that this maximum PLA length should not be exceeded for stealth characteristics. Experiments to delineate this more definitively are in progress.

Drug incorporation and release studies with one hydrophilic and one hydrophobic drug clearly showed that micelles formed from these copolymers clearly incorporate more hydrophobic drug, and control its release much more effectively. In particular, these systems may be used to encapsulate paclitaxel and to deliver it via parenteral administrations.

References

Avgoustakis, K., Beletsi, A., Panagi, Z., Klepetsanis, P., Ithankissios, D.S., 2002. PLGA–mPEG nanoparticles of cisplatin: in vitro nanoparticle degradation, in vitro drug release and in vivo drug residence in blood properties. J. Control. Rel. 79, 123–125.

Burt, H.M., Zhang, X.C., Toleikis, P., Embree, L., Hunter, W.L., 1999. Development of copolymers of poly(D,L-lactide) and methoxypolyethylene glycol as micellar carriers of paclitaxel. Colloids Surf. B: Biointerf. 16, 161–171.

Chabner, B.A., 1982. Pyrimidine Antagonists in Pharmacologic Principles of Cancer Treatment. Saunders, Philadelphia, pp. 132–142.

Crommelin, D.J.A., Storm, G., 1998. Targeting of drugs 6 strategies for stealth therapeutic systems. In: Bregoriadis, G., McCormack, B. (Eds.), NATO ASI Ser., Ser. A: Life Sci., 300, pp. 121–130.

Fu, Y.J., Shyu, S.S., Su, F., Yu, P.C., 2002. Development of biodegradable co-poly(D,L-lactic/glycolic acid) microspheres for the controlled release of 5-FU by the spray drying method. Colloids Surf. B: Biointerf. 25, 269–279.

Gref, R., Minamitake, Y., Peracchia, M.T., Trubetskoy, V., Torchilin, V., Langer, R., 1994. Biodegradable long-circulating polymeric. Nanospheres Sci. 263, 1600–1603.

Gref, R., Domb, A., Quellec, P., Blunk, T., 1995. The Controlled intravoues delivery of drug using PEG-coated sterically stablized nanospheres. Adv. Drug. Deliv. Rev. 15, 215–233.

Hagan, S.A., Coombes, A.G.A., Dunn, S.E., Davies, M.C., Illum, L., Davis, S.S., 1996. Polylactide-poly(ethylene glycol) copolymers as drug delivery systems.1. Characterization of water dispersible micelle-forming systems. Langmuir 12, 2153–2161.

Hu, D.S.G., Liu, H.J., 1994. Structural-Analysis and degradation behaviour in polyethylene-glycol poly (L-lactide) copolymers. J. Appl. Polym. Sci. 41, 473–482.

Jaeghere, F.De., Alllemann, E., Feijen, J., Kissel, T., Doelker, E., Gurny, R., 2000. Freeze-drying and lyopreservation of diblock and triblock poly(lactid acid)-poly(ethylene oxide) (PLA-PEO) copolymer annoparticles. Pharm. Dev. Technol. 5, 473–483.

Kim, S.C., Kim, D.W., Shim, Y.H., Bang, J.S., Oh, H.S., Kim, S.W., Seo, M.H., 2001a. In vitro evaluation of polymeric micellar paclitaxel formulation toxicity and efficacy. J. Control. Rel. 13, 191–202.

Kim, S.Y., Kim, J.H., Kim, D., An, J.H., LEE, D.S., Kim, S.C., 2001b. Drug-releasing kinetics of MPEG/PLLA block copolymer micelles with different PLLA block lengths J. Appl. Polym. Sci. 82, 2599–2605.

Leenslag, J.W., Gogolewski, S., Pennings, A.J., 1984. Resorbable materials of poly(L-lactide). V. Influence of the structure on the mechanical properties and hydolisability of PLLA fibres procedures by a dry spinning method. J. Appl. Polym. Sci. 29, 2829–2842.

Li, S.M., Rashkov, I., Espartero, J.L., Manolova, N., Vert, M., 1996. Synthesis, characterization, and hydrolytic degradation of PLA/PEO/PLA triblock copolymers with long poly(L-lactic acid) blocks. Macromolecules 29, 57–62.

Li, S.M., Anjard, S., Rashkov, I., Vert, M., 1998. Hydrolytic degradation of PLA/PEO/PLA triblock copolymers prepared in the presence of Zn metal or CaH_2. Polymer 39, 5421–5430.

Liggins, R.T., Burt, H.M., 2002. Polyether–polyester diblock copolymers for the preparation of paclitaxel loaded polymeric micelle formulations. Adv. Drug Deliv. Rev. 54, 191–202.

Matsumoto, J., Nakada, Y., Sakurai, K., Nakamura, T., Takahashi, Y., 1999. Preparation of nanoparticles consisted of poly(L-lactide)-poly(ethylene glycol)-poly(L-lactide) and their evaluation in vitro. Int. J. Pharm. 185, 93–101.

Nakada, Y., Tudomi, R., Sakurai, K., Takahashi, Y., 1998. Evaluation of long-circulationg nanoparticles using biodegradable ABA triblock copolymers containing of poly(L-lactic acid) A-blocks attached to central poly(oxyethylene) B-blocks in vivo. Int. J. Pharm 175, 109–117.

Okano, T., Yui, N., Yokoyama, M., Yoshida, R., 1994. In Advance in Polymeric Systems for Drug Delivery. Gordon and Breach Science, Yverdon, Switzerland, 24–66.

Onetto, N., Dougan, M., Hellmann, S., Gustafson, N., Burroughs, J., Florezyk, A., Canetta, R., Rozenweig, M., 1995. Safety profile. In: McGuire, W.P., Rowinsky, E.K. (Eds.), Paclitaxel in Cancer Treatment. Marcel Dekker, pp. 175–186.

Rashkov, I., Manolova, N., Li, S.M., Espartero, J.I., Vert, M., 1996. Synthesis, characteriazation and hydrolytic degradation of PLA/PEO/PLA Triblock copolymers with short poly(L-lactic acid) chains. Macromolecules 29, 50–56.

Riley, T., Govende, T., Stolinik, S., Xiong, C.D., Garnett, M.C., Illum, L., Davis, S.S., 1999. Colloidal stability and drug incorporation aspects of micellar-like PLA–PEG nanoparticles. Colloids Surf. B: Biointer. 16, 147–159.

Ruan, G., Feng, S.S., 2003. Preparation and characterization of poly(lactic acid)–poly(ethylene glycol)–poly(lactic acid) (PLA–PEG–PLA) microspheres for controlled release of paclitaxel. Biomaterials 24, 5037–5044.

Storm, G., Belliot, S.H., Daemen, T., Lasic, D.D., 1995. Surface modification of nanoparticles of nanoparticles to oppose uptake by the mononuclear phagocyte system. Adv. Drug Del. Rev. 17, 3–48.

Tadros, Th.F., Vincent, B., 1980. Influence of temperature and electrolytes on the adsorption of poly(ethylene oxide)-poly(propylene oxide) block copolymer on polystyrene latex and on the stability of the polymer-coated particles. J. Phys. Chem. 84, 1575–1580.